Formation of Volatile Organic Compounds in the Heterogeneous Oxidation of Condensed-Phase Organic Films by Gas-Phase OH

ARTICLE *in* THE JOURNAL OF PHYSICAL CHEMISTRY A · MARCH 2008

Impact Factor: 2.69 · DOI: 10.1021/jp0772979 · Source: PubMed

3 AUTHORS, INCLUDING:

A. Vlasenko
University of Toronto
52 PUBLICATIONS **872** CITATIONS
SEE PROFILE

Jonathan Abbatt
University of Toronto
279 PUBLICATIONS **6,498** CITATIONS
SEE PROFILE

Formation of Volatile Organic Compounds in the Heterogeneous Oxidation of Condensed-Phase Organic Films by Gas-Phase OH

Alexander Vlasenko, Ingrid J. George, and Jonathan P. D. Abbatt*

Department of Chemistry and Southern Ontario Centre for Atmospheric Aerosol Research, University of Toronto, 80 Saint George Street, Toronto, Ontario M5S 3H6, Canada

Received: September 11, 2007; In Final Form: December 6, 2007

The yield of volatile organic compounds (VOCs) from the heterogeneous oxidation of condensed-phase organic and hydrocarbon soot films by gas-phase OH has been studied in a coated-wall flow tube at room temperature. Simultaneously, OH concentrations are measured using a chemical-ionization mass spectrometer (CIMS) operated in negative ion mode and VOCs are measured using a commercial proton-transfer-reaction mass spectrometer (PTR-MS). It is observed that a variety of aldehydes/carbonyls and carboxylic acids are formed. Specifically, detailed experiments were conducted with stearic acid, where products are observed that contain as many as 13 carbon atoms with the average carbon number of the products between 3 and 5. The yield of VOCs, relative to the loss of OH radicals, is strongly dependent on the partial pressure of O_2 in the carrier gas, ranging from 0.08 ± 0.03 in a nominally pure He carrier gas to 0.34 ± 0.14 in 6 Torr of pure O_2. Yields from other organics are somewhat lower than those from stearic acid, ranging in conditions of pure O_2 from 0.10 ± 0.04 for BES (bis(ethylhexyl)sebacate), to 0.03 ± 0.01 for *n*-hexane soot, to 0.01 ± 0.005 for pyrene. Under atmospheric conditions, OH oxidation of select organics may be an efficient source of small VOCs. In particular, formic acid is formed in significant yield from all the surfaces.

Introduction

Given that OH is known to readily oxidize gas-phase organic molecules, it is not surprising that the heterogeneous loss of OH on organic surfaces has been shown to be highly efficient. Indeed, OH loss experiments conducted with 1-hexanol adsorbed on solid ammonium sulfate and with a variety of pure organics indicate that the reactive uptake coefficient for such interactions is larger than 0.2.[1,2] Recent experiments that monitor the loss of condensed-phase organics in submicron-size particles indicate that these gas-surface reactions proceed with close to unity efficiency.[3−6]

Unlike the kinetics, the products from OH heterogeneous oxidation are not nearly so well characterized, in part because they are likely to be strongly dependent on the chemical nature and phase of the condensed-phase organic, and also on the environmental conditions under which the oxidation occurs. In addition, there is the likelihood that some of the products will be sufficiently small so as to volatilize under experimental conditions whereas others will be large enough with many oxygenated functional groups that they will remain partitioned to the aerosol instead. In this paper, we perform what we believe is the first quantitative study of the yields of specific VOCs that are formed from such interactions.

From the perspective of atmospheric chemistry, the motivation for studying OH heterogeneous chemistry is not because this is an important loss process for OH; i.e., the gas-phase chemistry proceeds too fast for gas-particle loss to be of importance. Instead, the chemistry is important if it modifies the chemical character of the aerosols or gives rise to volatile products.[7] By following the loss of chemical tracers, Robinson et al. have inferred from field data that there is some degree of organic aerosol oxidation that occurs under photochemically active periods.[8] The potential importance of this modification is that the oxidized organic particles become more hygroscopic, thus increasing their probability for loss via wet deposition. Their radiative properties may change as well. From the gas-phase perspective, if OH chemistry drives a substantial amount of aerosol volatilization, then the products themselves could be of atmospheric relevance.[9] Also, it has been suggested that highly efficient volatilization may even lead to complete aerosol loss, at a rate competitive with other aerosol loss processes such as wet and dry deposition.[10]

This work extends that of others. As mentioned above, the kinetics of gas-phase free-radical loss on organic surfaces have been studied by a number of groups.[1−6,10−19] A general conclusion is that all radicals react more efficiently on a per collision basis than they do via gas-phase processes. From the product analysis perspective, there are very few studies with the focus being more on loss of the amount of condensed-phase material instead of direct determination of specific products. It is universally observed that there is a reduction in the thickness of self-assembled monolayers, such as octadecyltrichlorosilane (OTS), via oxidation by OH, Cl, Br and NO_3 radicals, but there is disagreement as to the degree of volatilization that occurs with some reports of only minor loss of carbon under atmospheric exposures. On the other hand, the work of Molina et al.[10] involving the direct exposure of OH to such films is commensurate with a significantly higher degree of volatilization, with only 2 or 3 OH collisions required to react away a saturated organic species containing 18 carbon atoms.[10] In the work of Molina et al., it is reported that HO_2, H_2O_2, CO, CO_2, HCO, CH_2O, CH_3CHO, CH_2OH and HCOOH are formed in the gas phase, but no specific yields are given. The condensed

* To whom correspondence should be addressed. Phone: (416) 946-7358. E-mail: jabbatt@chem.utoronto.ca.

10.1021/jp0772979 CCC: $40.75
Published on Web 01/29/2008

phase is observed to become increasingly oxidized in all studies, whether interrogated by infrared, mass spectrometric, or XPS techniques.

Our focus in this study is to both identify and quantify the formation of VOCs from the OH-driven oxidation of specific condensed-phase organics, including stearic acid, BES, pyrene, and *n*-hexane soot. These materials were chosen because they were all quite chemically reduced and so will be susceptible to OH oxidation. In addition, they are all of low volatility and so we can be confident that the chemistry in the flow tube is dominated by gas-surface and not gas-phase processes. Indeed, it is for this reason that pure saturated hydrocarbons are not used in this work, because of their relatively high vapor pressure. Stearic acid (SA) was chosen so that its long alkyl chain could act as a surrogate for the large hydrocarbon components of fresh diesel soot emissions. Also, surfactants of this type are found on the surfaces of natural bodies of water. BES is also a molecule that is largely chemically reduced, but it has a different phase (i.e., liquid) compared to stearic acid, which is a solid at room temperature. Pyrene was selected as an example of a polycyclic aromatic hydrocarbon that is known to partition to the surfaces of urban aerosols to a considerable degree.[20] Last, *n*-hexane soot has been recommended for study as a surrogate of black carbon in the atmosphere, given the elemental composition and high degree of aromaticity that it contains.[21]

Although quantitative yields of specific VOC production are needed to assess the atmospheric importance of this chemistry, they are as yet lacking in the literature. And so, the approach we have taken is to couple two mass spectrometers to a coated-wall flow tube so that we can simultaneously quantify the OH flux to the organic film, using a CIMS system operated in negative ion mode, and the VOC flux from the film using PTR-MS. An important point is that the similarity of the detection efficiencies of a wide range of oxygenated VOCs by the PTR-MS technique allows us to quantify the overall VOC yield, even if a wide range of products is observed. We are interested in the mechanism of the heterogeneous oxidation that will prevail in the atmosphere and so we pay attention to the environmental conditions by quantifying the yield as a function of O_2 and NO concentrations in the flow tube for the case of one organic, stearic acid. To compare the impact of chemical structure and phase on the chemistry, the overall VOC yields are then reported for a similar set of operating conditions for the other organics. We also study the evolution of the speciated VOC yield as the surfaces become increasingly oxidized.

Experimental Section

The coated-wall flow reactor has been described in detail elsewhere and so only a brief description is given here.[22] In addition, our approach to measurement of product yields from OH heterogeneous loss is given in Frinak and Abbatt, where we quantified the formation of Br_2 from exposure of gas-phase OH to bromide-containg solutions in a wetted-wall flow tube.[23]

We coat the inner walls of a 1.8 cm i.d. pyrex tube with stearic acid (Fisher Scientific) by briefly dipping the tube into a graduated cylinder containing the molten organic. The excess material on the exterior of the tube is removed whereas the inner surface appears to the eye to be uniform and smooth. For BES (Fluka), which is a liquid, a few milliliters are used to totally coat the inner walls of the pyrex tube, by rotating the tube a number of times. BES is sufficiently viscous that the coating remains over the entire surface during the course of an experiment. Although the liquid drains slowly to the bottom of the tube giving rise to a film of nonuniform thickness, we do not believe this affects the chemistry, which occurs only at the surface of the film. The pyrene coating is prepared in a similar manner using pyrene solution in dichloromethane. Inner walls are wetted with 3−5 mL of the solution. The tube is then rotated and the solvent is evaporated using dry nitrogen. The soot films are prepared using the flame from a sooting *n*-hexane flame according to the approach described in Aubin and Abbatt.[24] BET adsorption experiments indicate the films have a total surface area that is 75 times their geometric surface area. The elemental carbon (EC) content of such films, relative to the total carbon content, is about 95%.[24]

Once coated, the pyrex tube is placed within a low-pressure flow tube through which a carrier gas flows en route to a large rotary pump. Typical flow velocities are 4−10 m/s, and flow tube pressures are between 5.9 and 6.1 Torr.

OH radicals are formed from the fast reaction ($k_1 = 1.3 \times 10^{-10}$ cm^3 molecule^{-1} s^{-1}):[25]

$$H + NO_2 \rightarrow OH + NO \quad (1)$$

In particular, H atoms are generated in a microwave-induced plasma through which is passing a 50 sccm of Ar containing a trace amount of H_2 (BOC). The H-atom-containing flow passes to the flow tube through 50 cm of 0.318 cm o.d. Teflon tubing that runs down the center of a 0.4 cm i.d. movable glass injector. Between the outside of the Teflon tube and inner walls of the injector, we pass a small flow of NO_2 (Matheson), metered from a dilute mixture in N_2 contained in a large glass bulb. Typical NO_2 concentrations in the flow tube are $(3-7) \times 10^{11}$ molecules/cm^3. We operate the experiment in a mode where the H atom concentration is close to or in excess of that of the NO_2. By observing the change in the NO_2 CIMS signal when the microwave discharge is on versus when it is off, we are measuring the production rate of OH radicals in the flow tube under the assumption that the loss of each NO_2 molecule is caused by reaction 1. We estimate the uncertainty in the concentration of OH to be on the order of ±25%.

Downstream of the coated pyrex tube are two mass spectrometry systems. The first is a home-built, negative-ion CIMS that samples the flow through a pinhole and two stages of differential pumping. Ions are formed at the flow tube pressure by passing 1 SLM of N_2 containing a trace amount of SF_6 (BOC) through a Po-210 radioactive source (NRD) before mixing with the carrier gas from the flow tube. Species in the flow react with SF_6^- by fast ion−molecule interactions ($k_2 = 2 \times 10^{-9}$ cm^3 molecule^{-1} s^{-1} and $k_3 = 1.3 \times 10^{-10}$ cm^3 molecule^{-1} s^{-1}):[26,27]

$$OH + SF_6^- \rightarrow OH^- + SF_6 \quad (2)$$

$$NO_2 + SF_6^- \rightarrow NO_2^- + SF_6 \quad (3)$$

The nitrogen dioxide CIMS signal was found to be linearly dependent on partial pressure in the range where the exposures were performed. The sensitivity for NO_2 was 3×10^{-8} counts s^{-1} cm^3 molecule^{-1}, calculated using the ratio between the signal for NO_2 and SF_6. The typical SF_6^- signal was 300 000 counts s^{-1}. Typical background signals at masses *m*/*z* 17 (OH^-) and 46 (NO_2^-) were 10 and 16 cps, respectively. The origin of these background counts is mostly electronic noise. From the background signal at *m*/*z* 46 and from calibrations with known flows of NO_2, we calculate that the detection limit is about 10^9 molecules cm^{-3} for NO_2 for 1 s integration time (S/N =1).

The PTR-MS instrument (Ionicon Inc.) used in this work was acquired from Ionicon Analytic (for detailed description see

Lindinger et al.).[28] To detect oxygenated VOCs (OVOC), the PTR-MS also sampled the flow, through a Teflon on−off valve and 165 cm of 0.63 cm o.d. Teflon tubing:

$$H^+\cdot H_2O + OVOC \rightarrow H^+\cdot OVOC + H_2O \qquad (4)$$

In particular, the PTR-MS ion source is tuned to produce very high concentrations of the H_3O^+ reagent ion, which readily donates a proton to species—including all oxygenated organics—that have a proton affinity higher than that of water. To maintain the appropriate pressure in the drift tube region of the mass spectrometer, we bypassed the entire inlet system of the commercial PTR-MS unit and instead connected the 0.63 o.d. Teflon tube directly to the drift region. We estimate that roughly 15 sccm of flow was sampled by the PTR-MS. Another change from the normal operation of the PTR-MS system is that we used pure oxygen as the carrier gas in the flow tube at times. As a result, the voltages of the ion lenses in the mass spectrometer system had to be changed to maximize the reagent ion signal for each carrier gas composition. The intensity of the H_3O^+ signal was on the order of 10^7 counts s^{-1}, as determined from the measured signal at *m*/*z* 21 and using isotopic abundances. Even with pure oxygen as the carrier gas, the level of O_2^+ was no more than 7% of the H_3O^+ signal, ensuring that the vast majority of the ionization was occurring via H_3O^+ and not O_2^+.

To calibrate the PTR-MS, we used three small VOCs: propanol (ACP Chemicals), acetic acid (Fisher Scientific), and hexanal (Aldrich). In each case, a dilute mixture in N_2 was prepared in a glass bulb from a freeze−pump−thaw cycle, and a measured flow was delivered into the coated-wall flow tube for the calibration. Calibrations were conducted at each overall He (Grade 5, BOC) to O_2 (Grade 4.4, BOC) composition of the carrier gas. For acetic acid, the effects of gas-phase dimerization were taken into account by using the literature equilibrium constant to calculate the relative proportions of monomers and dimers in the glass reservoir at the measured pressure.[29] The total flow of acetic acid molecules from the reservoir was then determined by taking into account that each dimer contributed two acetic acid molecules to the flow tube.[30] As expected, it was found that the calibration factors for acetic acid and hexanal were very close to each other, to within ±15%. A small degree of fragmentation of protonated molecular ion, via loss of H_2O, was observed for acetic acid. Expressed as a percentage of total signal intensity arising from the fragment this corresponded to 20% and 10% in flow of helium and oxygen flows, respectively. By comparison, there was extensive fragmentation of protonated hexanal (60%) and complete fragmentation of protonated propanol (100%). Typical detection limits for acetic acid and hexanal were roughly 10^9 molecules cm^{-3} in the flow tube. Note that we apply the average of the calibrations of hexanal and acetic acid to determine the yields of all the VOCs. Given that the rate of reaction 4 is at the ion−molecule collision rate for most species, we believe this calibration to have an accuracy of roughly ±30% for calculating the sum of the OVOCs formed.

Results

i. OH Decay. Although this was not the focus of our experiments having been studied previously,[2] we nevertheless observed via the CIMS signal at *m*/*z* 17 that OH reacts rapidly with the condensed-phase films. Most of the measurements in this paper were performed by positioning the injector well upstream, exposing the radicals to the full coating length of the coated-wall surface. Under these conditions, where OH experiences many collisions with the wall, the signal of OH decays to background levels as a result of surface loss, relative to the value it exhibits with the injector tip pushed in well upstream of the coated pyrex tube. In other experiments, where OH is exposed to a considerably shorter length of the film and the exposure time was only a few milliseconds, the experimentally measured decay of OH was close to that for gas-phase diffusion-limited wall loss. This is in agreement with the diffusion-controlled kinetics observed for heterogeneous loss of OH radicals.[1,2]

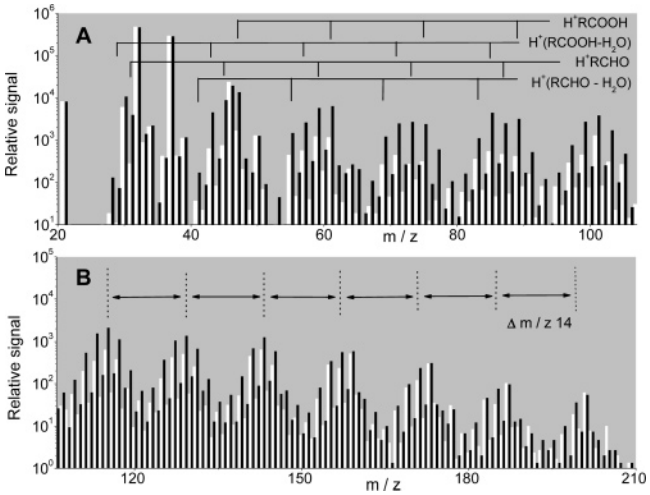

Figure 1. PTR-MS spectra of gas-phase species formed in the surface reaction of stearic acid and OH (black columns) and background measurements in the absence of OH radicals (white columns). The spectra are split into two panels for different mass ranges. Carrier gas flow is oxygen.

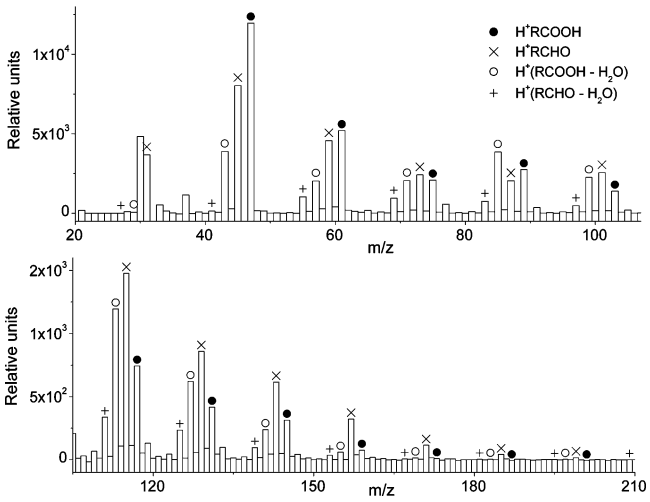

Figure 2. PTR-MS difference spectrum for oxidation of SA coating calculated by subtracting the background spectrum from that when OH is exposed to the surface. Peaks at *m*/*z* 32 and 46 are negative and not shown (see explanation in text). The spectra are split into two panels to represent different mass ranges. The signs above specific masses correspond to identified peaks in sequences A, B, A-H_2O, and B-H_2O (see explanation in text). Carrier gas flow is oxygen.

ii. VOC Products. The formation of volatile gas-phase products from heterogeneous surface oxidation of stearic acid is shown in Figure 1, where the PTR-MS spectrum measured with the OH radical present in the reactor, i.e., the microwave plasma is on, is compared to that measured in the absence of OH, i.e., the microwave is off. The injector is maintained at a constant position, and the products reach steady-state concentration at a time scale faster than a PTR-MS scan (which typically

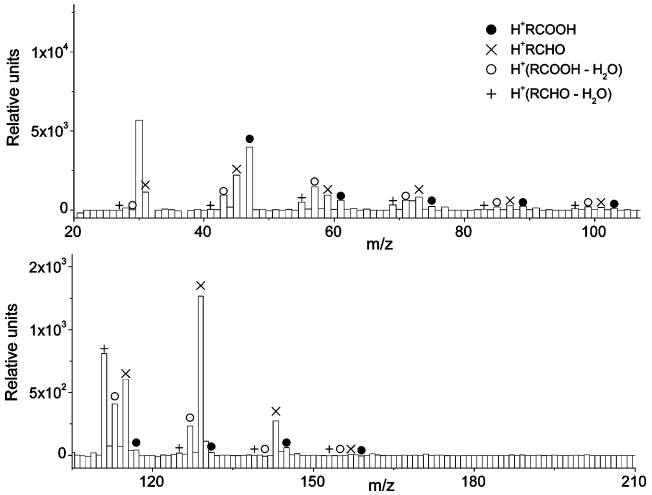

Figure 3. PTR-MS difference spectrum for oxidation of BES surface. Carrier gas flow is oxygen.

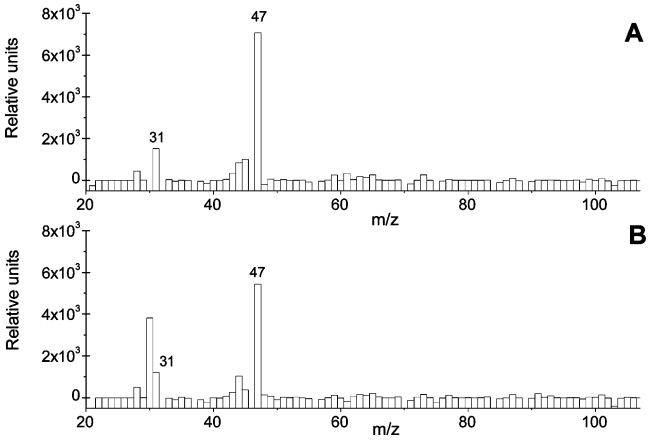

Figure 4. PTR-MS difference spectrum for oxidation of soot (panel A) and pyrene (panel B) surfaces. Carrier gas flow is oxygen.

takes 230 s). Each spectrum is an average of five consecutively measured full scans of the quadrupole up to 230 amu. The overall time to make these observations is on the order of 20 min with the microwave on. For better representation of the data, a difference spectrum between mass spectra recorded with OH present versus those with OH absent is plotted in Figure 2 for stearic acid and in Figures 3 and 4 for BES, pyrene and *n*-hexane soot, respectively.

The largest peaks in Figure 1, at *m*/*z* 21, 32 and 37, correspond to H_3O^+, O_2^+ and $H_3O^+ \cdot H_2O$, respectively. The intensities of these peaks are not significantly changed in the presence and absence of OH radicals. Peaks at *m*/*z* 30 and 46 correspond to NO^+ and NO_2^+, respectively. Formation of these ions may be proceeding through charge exchange with O_2^+. The change of the intensities of these peaks is due to the conversion of NO_2 to NO as a result of H-atom titration. Note that because the intensities of O_2^+ and NO_2^+ are higher when OH is not present in the reactor, the differences are negative and are not plotted in Figures 2−4.

We attribute all other changes in the mass spectrum as arising from OH surface oxidation chemistry. In particular, the intensity of some specific peaks is increased by almost a factor of 10 as a result of the OH exposure. This indicates that volatile gas-phase products are being formed and then detected downstream of the reaction zone. Note that the background peaks in the absence of OH arise from impurities/degassing in the flow tube, or along the Teflon line leading to the PTR-MS. It is not

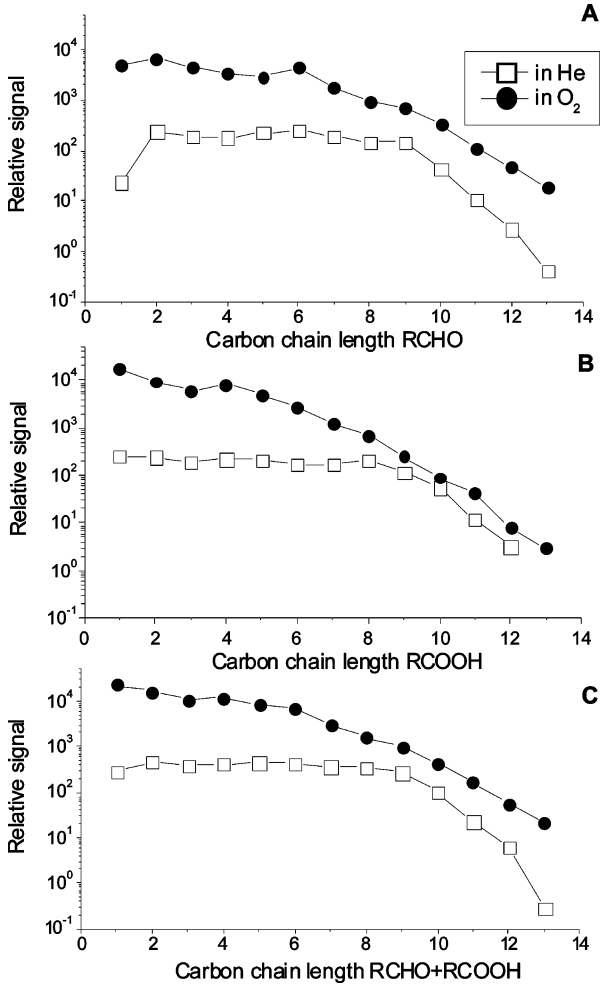

Figure 5. Relative abundance of volatile products as a function of carbon chain length. Panel A: aldehyde/ketones. Panel B: carboxylic acid. Panel C: sum of the species. Reaction of OH with SA coating in oxygen as carrier flow.

surprising that they arise at some of the same masses as those observed for the oxidation products because, as described below, the products represent a very wide suite of carboxylic acids and carbonyls, which are likely VOC impurities that might be present.

Considering each difference spectrum separately, we see for stearic acid that there is some regularity in the mass position of the peaks showing increased intensity with OH exposure. The difference of 14 amu in the mass-to-charge ratio indicates that the volatile products differ in structure by a CH_2 group; i.e., the products have the same chemical nature but have different carbon chain lengths. In particular, within the spectrum we see a sequence of peaks (which we will refer to as sequence A) that are consistent with either protonated aldehydes or carbonyls *m*/*z* of 31, 45, 59, 73, ... Also, an independent sequence (sequence B) arises from protonated carboxylic acids, aldehydic carboxylic acids, or alcohols, at *m*/*z* 47, 61, 75, 89, ... For each of these sequences, we also observe complementary sequences (sequence A-H_2O and sequence B-H_2O) that correspond to the fragment formed by the loss of water from the protonated oxygenated organics, i.e., from the aldehyde/carbonyl sequence, there is intensity at *m*/*z* 41, 55, 69, 83, ..., and with the carboxylic acid/alcohol sequence there are peaks at *m*/*z* 43, 57, 71, 85, ...

The abundance of volatile reaction products as a function of carbon chain length and amount of O_2 in the carrier gas is shown in Figure 5. The average C-number (i.e., carbon chain length,

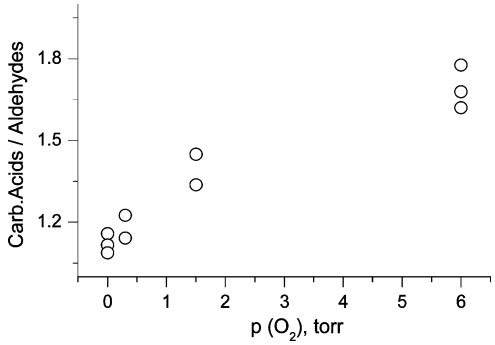

Figure 6. Ratio of the yield of volatile carboxylic acids to aldehydes is presented as a function of the oxygen partial pressure in the reactor from heterogeneous reaction of OH with SA.

l) of the products is calculated according to

$$l = \frac{\sum i \cdot [\mathrm{VOC}]_i}{\sum [\mathrm{VOC}]_i} \quad (5)$$

where i is a number of carbons in the molecule and $[\mathrm{VOC}]_i$ is the concentration of molecules with i carbons. When the carrier gas is pure He with only a trace amount of O_2 present, products with one to nine carbons (i.e., C1 to C9) are formed with similar yield. The formation of molecules larger than C9 is not as significant, most likely due to their decreased volatility. Overall, the average number of carbon atoms in the product molecules is 5.1. At higher oxygen partial pressures, there is a tendency for shorter molecules to be formed over the time scale at which these experiments are performed. The average number of carbon atoms in the products changes to 3.2 in this case. The relative yield of carboxylic acids/alcohols (sequences B and B-H_2O), referenced to aldehydes/carbonyls (sequences A and A-H_2O), is strongly dependent on the partial pressure of oxygen, rising above unity when there is more than trace oxygen in the carrier gas (see Figure 6).

For each of BES, pyrene and *n*-hexane soot, the clear progression of product peaks observed with stearic acid is absent. Instead, the products are localized into a smaller number of peaks, with intensity at small mass products dominating the spectra. This is particularly true for pyrene and *n*-hexane soot where the only signals that are clearly identified above background levels are at *m*/*z* 47 and 31, consistent with the formation of formic acid and formaldehyde. For BES, there is significant intensity at *m*/*z* 129 and *m*/*z* 111, which corresponds to the formation of ethylhexanal as discussed later.

Note that although Figures 2−4 show results for pure O_2 carrier gas, similar profiles of product peaks are exhibited with lower partial pressures of oxygen present as well, including nominally pure helium.

iii. VOC Yields. To calculate the flux of OH to the coated-wall surface, not only do we need to calculate the generation rate of OH (as mentioned in the Experimental Section) but we also need to assume that every OH formed in the gas phase is lost heterogeneously rather than via a gas-phase process, such as via reaction with NO, NO_2 or itself. In our previous paper on the formation of Br_2 from reactive uptake of OH by bromide-containing solutions, we have shown that this gas-phase chemistry is substantially slower than the heterogeneous loss rate, assuming gas-phase diffusion-limited loss of OH to the wall.[23] Indeed, the flow tube in our earlier study was operated with higher pressure and slower overall flow velocities than the current study, and so we expect that wall-loss kinetics will be even more dominant in this work. Note that in that study we measured yields of Br_2 relative to OH loss that are consistent with the known mechanism for such chemistry in solution, thus validating this overall approach for quantification of gas-phase product yields from OH in coated-wall flow tubes. To be specific for the conditions of this experiment, OH is lost within a very short distance within the flow tube, i.e., typically within 3 ms of injection into the flow tube, as determined by the gas-phase, diffusion-controlled loss rate. This corresponds to a first-order wall-loss rate constant order of 3×10^2 s^{-1}. For gas-phase chemistry to occur with the same kinetics, gas-phase species must be present at a concentration of 3×10^{13} molecules/cm^3, assuming a (fast) gas-phase rate constant between OH and the organics of 1×10^{-11} molecules/cm^3. This is highly unlikely, as the reactants (stearic acid, pyrene and BES) have room-temperature vapor pressures of less than 2×10^{11} molecules/cm^3.

We define the volatile product yield (Y) as the ratio of the total volatile gas-phase product concentration to the concentration of OH radicals that have reacted:

$$Y = \frac{\Delta[\mathrm{VOC}]}{\Delta[\mathrm{OH}]} = \frac{\sum [\mathrm{VOC}]_i}{\Delta[\mathrm{OH}]} \quad (6)$$

The total concentration of VOCs produced in the reaction is calculated as a sum of individual $[\mathrm{VOC}]_i$ concentrations derived from the PTR-MS measurements. Note, however, that the PTR-MS is insensitive to CO and CO_2 and has low sensitivity to some alcohols. In that way, the yields we report are specifically for the OVOCs to which the PTR-MS is sensitive. The concentration of OH that has been reacted is equal to the initial concentration of OH, because the radicals are only removed by collision with the surface. As described in the Experimental Section, we assume the initial OH concentration to be equal to the change in NO_2 concentration arising from the microwave being turned off and on. Overall, given the potential errors in both the OH and OVOC measurements, we estimate our overall uncertainties in the reported yields are certainly less than a factor of 2 and probably closer to a factor of 1.5.

The product yields for stearic acid are shown in Table 1, where a strong dependence on the concentration of O_2 in the flow tube is demonstrated with greater yield in pure O_2 (6 Torr). To compare the yields measured between different films, we also measured the VOC yields from BES, pyrene and *n*-hexane soot under a common set of conditions of high and low O_2 partial pressure. In oxygen we find the yields are considerably reduced relative to those from stearic acid, with the overall values being 0.1 for BES, and 0.03 *n*-hexane soot for and 0.01 for pyrene. For comparison under similar conditions, the yield from stearic acid is 0.34. In helium, the yields overall are lower: 0.08 for SA and BES and below 0.02 for pyrene and *n*-hexane soot. The purity of the helium used is 99.999%, which suggests that $O_2 \leq 10^{-4}$ Torr when pure He is flowing.

iv. Heterogeneous Oxidative Aging. To investigate the effect of surface aging on the formation of VOCs, a short fragment of film about 1 cm in length was exposed to a constant concentration of OH radicals for about 2 h (Figures 7−9). As shown by time periods without data, the generation of OH was stopped during the experiment to measure the background signals, to ensure they were smaller than the signals observed with OH exposure. For stearic acid and BES the volatile product yield was observed to decrease with OH exposure, but even after 2 h of exposure there was still clear formation of products. For the *n*-hexane soot and pyrene surfaces we observed a small, steady increase in the yield with time.

TABLE 1: OVOC Product Yields

	in oxygen			in helium		
surface	[VOC][b]	[OH][b]	Y[c]	[VOC]	[OH]	Y
stearic acid	23.7 ± 0.2	69 ± 2	0.34 ± 0.14	1.70 ± 0.05	22 ± 2	0.08 ± 0.03
BES	5.8 ± 0.1	57 ± 1	0.10 ± 0.04	1.35 ± 0.04	17 ± 1	0.08 ± 0.03
hexane soot	1.55 ± 0.05	60 ± 2	0.03 ± 0.01	<0.1[d]	23 ± 1	<0.005
pyrene	0.60 ± 0.04	42 ± 1	0.014 ± 0.006	<0.1[d]	20 ± 1	<0.005

[a] Concentrations are in units of 10^{10} molecule cm^{-3}. [b] Values shown are mean and $\pm 1\sigma$ precision uncertainties. [c] Y is the VOC yield, relative to OH loss; indicated errors are one least-squares standard deviations combined with estimated overall uncertainties. [d] [VOC] measured is below detection limit 1×10^9 molecule cm^{-3}.

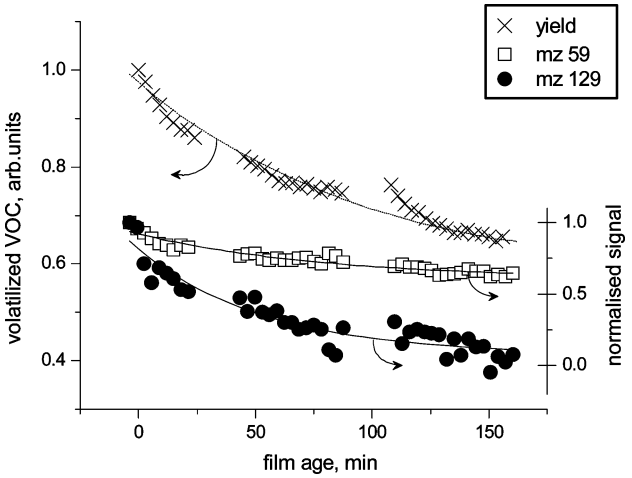

Figure 7. Volatile product yield (crosses) as function of SA film age, i.e., exposure time. Gas-phase concentrations of short (open boxes) and long (solid circles) volatile products are presented as ion signals of *m*/*z* 59 and 129, respectively, normalized to initial values. The lines are plotted to guide the eye.

Discussion

A key observation from this work is that the VOC products and their respective yields are highly dependent upon the chemical nature of the film and/or its physical phase. Stearic acid is a solid at room temperature with a long hydrocarbon chain. Given the high VOC yields, it is clear that carbon−carbon bonds in the molecule can be easily broken, under appropriate environmental conditions of sufficient O_2. On the other hand, pyrene and *n*-hexane soot, which are also highly chemically reduced, exhibit substantially lower VOC yields. BES represents an intermediate case where the yield is close to 0.1. To discuss the chemistry in more detail, we use a reaction mechanism that is based on gas-phase alkane oxidation schemes and other recent papers[10,14,16−18] (see Figure 10). We initially discuss the chemistry that occurs with stearic acid given the wide range of experiments we conducted with it. We then discuss how the chemistry may differ with the other substrates.

i. Stearic Acid. The reaction sequence is initiated by H-atom abstraction and the formation of an alkyl radical (R) and gas-phase water. The formation of water is confirmed in our experiments by increase of peak intensity at *m*/*z* 37 in the PTR-MS spectrum. This arises from the $H_3O^+ \cdot H_2O$ complex, the intensity of which is strongly affected by gas-phase water amounts. The alkyl radical rapidly reacts with O_2, forming the peroxy radical (RO_2) that reacts with either NO or another RO_2 species, forming an alkoxy radical (RO). Alternatively, the RO_2 self-reaction may form an alcohol/carbonyl pair. Decomposition of alkoxy radicals leads to carbon−carbon bond scission and formation of an aldehyde and another alkyl radical, both of which have fewer carbons than the starting material. Alternatively, the RO radical may isomerize to form a hydroxyalkoxy radical, react with O_2 to form a carbonyl plus HO_2, or react with NO_x leading to nitrification of the surface. Note, however, that these pathways do not lead to C−C bond breakage.

For stearic acid, the C−C bond scission part of the mechanism implies the formation of either an aldehyde or aldehydic acid, matched to, respectively, either an alkyl radical with a carboxylic acid functional group at one end of the chain or a simple alkyl radical. If the products are sufficiently volatile, they could partition to the gas phase and be detected by the PTR-MS downstream of the reaction zone. Because the H-atom abstraction can occur at many CH_2 positions in the molecule, one can rationalize the two product series of peaks (i.e., sequences A/A-H_2O and B/B-H_2O) in the product mass spectrum that were detailed in the Results section, i.e., one corresponding to the formation of terminal aldehydes and the other to aldehydic acids.

However, one important uncertainty in this analysis is whether sequence B/B-H_2O corresponds to the formation of carboxylic acids, aldehydic acids, or alcohols, or to some combination thereof. All these species can have the same nominal mass that is unresolvable by the quadrupole in the PTR-MS instrument. Given that there is sizable intensity at *m*/*z* 29, 43, 47 and 61, which could arise from monocarboxylic acids or alcohols and their fragment peaks, but not from aldehydic acids, we know that aldehydic acids do not give rise to the intensity in all these masses. Indeed, given the absence of a large peak at the smallest mass that would correspond to a protonated alcohol (methanol, *m*/*z* 33) but significant intensity at the smallest monoacid (formic acid, *m*/*z* 47), we are inclined to believe that sequences B and B-H_2O have significant monocarboxylic acid contributions. This is also consistent with the low sensitivity that the instrument has to small alcohols, as shown in the calibration studies with propanol. In addition, short-chain carboxylic acids were also detected as products of hexadecane heterogeneous oxidation by OH/O_3 in NO_x free environment.[14] More detailed studies, using either an off-line chromatographic approach or an on-line experiment with high mass resolution, are required to be more definitive in this regard. A final point to note is the relative independence of the product signal in sequence B and sequence B-H_2O on the number of carbons in the product in the low O_2 studies (see Figure 5), which is suggestive that a common mechanism and set of products prevails across the length of the sequence, i.e., the monocarboxylic acids.

If monocarboxylic acids are indeed being formed in this chemistry, their formation mechanism is not clear. It seems unlikely that they could arise from the organic radical left on the surface abstracting a H-atom from another entity. It is more likely that oxidation of aldehydes on the surface could be driven by OH and HO_2. For example,[31]

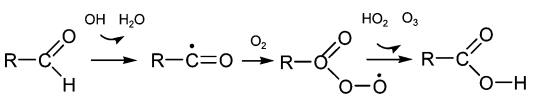

(7)

given that there will be some HO_2 in the flow tube as well as OH. Acylperoxy radicals, as formed in reaction 7, also undergo a reaction with HO_2 forming peroxyacids, which can ultimately yield carboxylic acids.[32,33] Another possibility for this reaction pathway is aldehyde hydration at the surface followed by diol oxidation:[34]

$$RCHO + H_2O \leftrightarrow RCH(OH)_2 \quad (8)$$

$$RCH(OH)_2 + OH + O_2 \rightarrow RCOOH + HO_2 + H_2O \quad (9)$$

Both of these mechanisms are dependent on the amount of O_2, and so it might be expected that the formation of carboxylic acids would be preferred over aldehydes at high O_2 levels. Indeed, the ratio of the intensity of products in sequence B/B-H_2O relative to those in sequence A/A-H_2O increases from 1.1 to 1.7 as the carrier gas changes from He to pure O_2 (Figure 6). We believe that the carboxylic acids are not being formed in the gas phase, from OH oxidation of aldehydes, given the much longer time scale for that chemistry compared to the rate of OH loss on the wall.

We note that the sum of all peaks within sequences A, B, A-H_2O and B-H_2O contribute at least 80% and 85% of the integral signal intensity in main flows of helium and oxygen, respectively. (For this calculation, intensities of peaks at *m*/*z* 21, 30, 32, 37 and 46 were excluded when calculating the integral signal intensity.) Unidentified signal intensity comes from peaks with *m*/*z* 44, 48, 60, 77 and 91, indicating that the chemistry is not as simple as that just described.

As one example, we note that organic nitrates could also be formed and volatilized in the surface reaction of stearic acid with OH, given that we have NO_x present. Formation of organic nitrates was observed earlier in the study of secondary aerosol formation from the reactions of *n*-alkanes with OH radicals in the presence of NO_x.[15] It is not known how these compounds could be detected with the PTR-MS, but we speculate that they fragment in a way similar to that observed for PAN giving product ions RO^+ or R^+.[35] There is also the potential for formation of other secondary oxidation products beyond the formation of carboxylic acids. For example, alkoxy radicals could react with oxygen forming a molecule with a carbonyl group. This molecule could then react with another OH, and the scission products could contain two or more oxygenated functional groups.

According to the gas-phase reaction mechanism NO could potentially shift the branching ratio toward formation of RO radicals and away from formation of alcohol/carbonyl products.[36] To test whether this was the case, we added NO to the main flow in experiments with both pure oxygen and pure helium carrier gas. The experiment in He showed that the VOC production is not affected by the addition of NO even up to relatively high NO concentrations (1×10^{13} molecules/cm^3), i.e., higher than those that would have been prevalent for the experiments presented in the paper. The test in O_2 showed just a slight increase (+10%) of OVOC production. Therefore, we conclude that NO concentrations used were high enough so that formation of alkoxy from RO_2 was not limited by NO.

Overall, for conditions of sufficient O_2, we observe VOC yields of 0.34 for SA, with the average number of carbon atoms in the products ranging from 3 to 5, depending on the carrier gas (see Results). This implies that between 9 and 15 OH collisions are required to remove one stearic acid molecule entirely. This is a higher result than that of Molina et al. who observed 2−3 OHs were needed to remove one C18 chain from a surface.[10] It should be noted, however, that the substrates are very different. The Molina et al. work was done with self-assembled monolayers, whereas ours was with a highly involatile fatty acid. From our work the yields are strongly dependent on the chemical nature of the substrate, which could explain some of the difference. Note that our studies were done at much higher OH concentrations, which might enhance the reaction pathway that proceeds via the RO_2 self-reaction. We note also that C−C bond scission seems to be quite enhanced for heterogeneous reactions given that it is reported to be minor for OH reactions with *n*-alkanes in the gas phase.[37,38] Finally, we note that the VOC yields are lower in the He buffer gas, with only trace O_2 present. We believe this is because the alkyl radicals formed by OH H-abstraction do not full react with the trace O_2. Instead, it is likely that a considerable degree of alkyl radical self-reaction will occur, giving rise to cross-linked products. Whether this occurs at lower OH fluxes would be interesting to investigate.

ii. Other Substrates. Whereas stearic acid yielded a sequence of products, arising because the OH could attack anywhere along its long alkyl backbone, we did not observe the same for BES, pyrene or soot. For BES, we observed significant product intensities at *m*/*z* 129 (MH^+) and *m*/*z* 111 ($MH^+ - 18$), which correspond to formation of 2-ethylhexanal, as would occur if OH attacked hydrogen in $-CH_2-O-$ position. A study of the OH + isobutyl acetate ester reaction in the gas phase has shown that H-atom abstraction is fastest at the α-CH_2 group.[39] If we assume a similar mechanism for heterogeneous OH + BES reaction, then the observed formation of 2-ethylhexanal could be described as following:

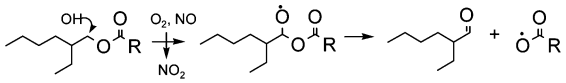

(10)

It is interesting that there is some selectivity in the products that are formed in this oxidation process. In particular, although the uptake coefficient for OH loss is close to unity, it does appear that the OH must undergo some degree of movement on the surface before reaction. Consistent with some degree of surface adsorption prior to reaction is that the unity uptake coefficient is larger than the corresponding reaction efficiency for collisions in the gas phase for species with alkane chains.

Why is the VOC yield considerably lower for BES than for stearic acid? In another study where we have used electrospray-MS and coupled SMPS/AMS analysis of oxidized BES particles,[4] we have shown that a major set of products in the BES system are alcohols and carbonyls arising either from the RO_2 self-reaction or from reactions of the RO radical. BES is a liquid and so it may be that the RO_2 self-reaction channel is promoted over the RO bond scission channel because of the ease of RO_2 self-reaction in a liquid where diffusion rates are rapid, versus in a solid where radicals may not so easily encounter each other. Indeed, the overall degree of volatilization inferred in the aerosol experiments[4] is roughly consistent with that observed here. BES particle mass change (as a function of OH exposure) is found to be a combination of density increase and volatilization.

For pyrene and *n*-hexane soot, there are very few gas-phase products. For pyrene, OH will react by adding to an aromatic ring, so forming a large surface organic radical, to which O_2 will then add. Although bond scission has been observed in the reaction of OH with gas-phase aromatics,[40,41] if carbon−carbon bond breakage occurs with pyrene, the resulting fragements will probably be sufficiently large that they will not volatilize. The same goes for a *n*-hexane soot surface as well, given that low molecular weight aromatics will have desorbed from its surface

in the flow tube. Indeed, with a soot-coated tube in the reactor, we observed in the background mass spectra intensity of relatively large PAHs, but not those at lower masses. Thus, it is likely that the OH reacts with these PAHs, with larger and less volatile ones, with other organics condensed on the soot, or with the graphitic backbone itself. Whatever the case, the products will be of high molecular weight and low volatility. That all being said, there was significant formation of intensity at *m*/*z* 47 and 31 for these substrates, corresponding most probably to the formation of formic acid and formaldehyde.

iii. Heterogeneous Oxidative Aging. To check the effect of surface aging on the formation of OVOC, a 1 cm length of the film was exposed to a constant flux of OH radicals for about 2 h. In the case of stearic acid, the volatile product yield decreased 30% during this time period (Figure 7). An explanation to this observation is that continuous oxidation is increasing the number of C=O and C−OH functional groups at the surface, and thus decreasing the volatility of potential products. Nevertheless, it is quite remarkable that even after about 2 h of aging, the film still exhibited a large VOC yield. In 1 second, we calculate that the flux of OH radicals that have collided with the surface (assuming it is smooth) is on the order of 10^{14} collisions/cm^2, similar to the number of stearic acid molecules present per cm^2. An experiment, however, is many minutes long and so it is clear that many stearic acid molecules are being oxidized during an exposure experiment, i.e., as products leave the surface, fresh stearic acid molecules become available for oxidation. [Note that even if the surface displays some surface roughness, this conclusion is still valid because it is unlikely that the stearic acid films have higher specific surface areas than our soot films, which we know to have 100 times more surface area than a flat surface.] Alternatively, a thin liquid layer forms on the surface containing the different reaction products, in which the stearic acid is soluble.

Another consequence of the stearic acid film aging is a considerable decrease of the formation of larger gas-phase products. For example, Figure 7 shows that after 2 h of film aging the signal measured at *m*/*z* 129 is less than 10% of the initial value. At the same time the signal at *m*/*z* 59 that corresponds to a shorter product molecule has decreased to a far smaller degree, 60% of initial value. We see similar behavior across the mass spectrum with the higher *m*/*z* signals decreasing at a considerably faster rate than the signals of lighter product molecules. This will arise via secondary chemistry involving OH attack on prior oxidation products. In particular, there is a greater likelihood of larger species being lost via reaction with OH than smaller species; i.e., there are more $-CH_2-$ groups to attack in the larger molecules.

The results for the oxidative processing of the BES surface are similar to those for stearic acid with the overall yields decreasing 40% of the initial value after 1.5 h of OH exposure. As the film becomes more oxidized, signal *m*/*z* 129 of longer product molecules decreases faster compared to that of a shorter molecule at *m*/*z* 59 (Figure 8). In the case of soot and pyrene the yields increase with time (Figure 9), albeit at a slow rate. The major part of this increase is the growth of formic acid production detected at *m*/*z* 47.

iv. Atmospheric implications. In this study we showed that organic surfaces react efficiently with OH radicals and some reaction products are sufficiently volatile to partition to the gas phase, thus corroborating the work of Molina et al.[10] Product yields are highly sensitive to the chemical nature of surface. With regard to an atmospheric organic aerosol particle this means that the chemical composition is a key parameter

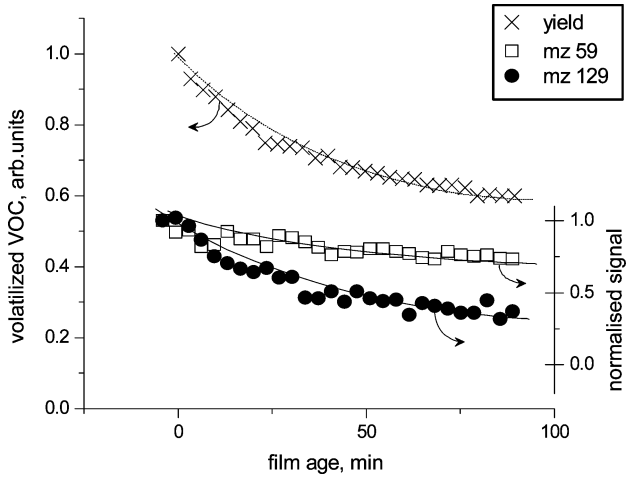

Figure 8. Volatile product yield (crosses) as function of DOS film age. Gas-phase concentrations of short (open boxes) and long (solid circles) volatile products are presented as normalized ion signals of *m*/*z* 59 and 129, respectively. The lines are plotted to guide the eye.

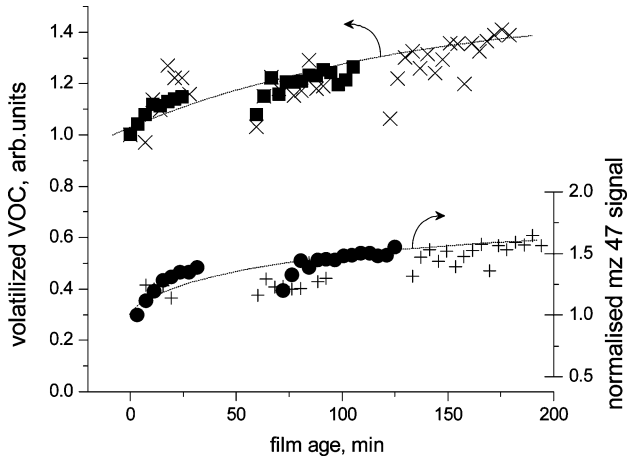

Figure 9. Volatile product yield as function of film age (soot, boxes; pyrene, crosses). Gas-phase concentrations of volatilized HCOOH presented as normalized ion signal of *m*/*z* 47 (soot, circles; pyrene, pluses). The lines are plotted to guide the eye.

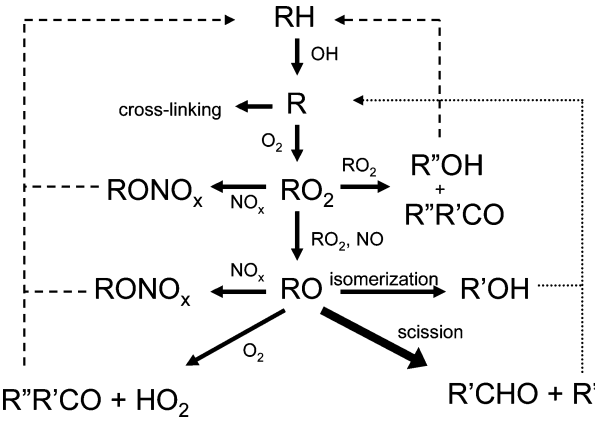

Figure 10. Proposed reaction mechanism for alkane surface oxidation by OH. The mechanism is based on gas-phase alkane oxidation schemes.

describing the degree of volatilization. For instance, soot particles are expected to undergo minor carbon loss during oxidative atmospheric aging. On the other hand, the saturated hydrocarbon component of an aerosol should be more susceptible to volatilization according to results of this study. It should be mentioned that the oxidation conditions of our experiments

are different from the typical atmospheric environment so that one should extrapolate experimental findings with caution. Higher concentrations of OH used in this study could possibly explain lower volatilization of SA film compared to the previous work.[10]

Not only particle composition but also the physical state could be important to describe volatilization initiated by OH. Data suggest that volatile product yield is three times higher for solid SA compared to liquid BES. This may be due to an enhanced RO_2 recombination mechanism in the liquid phase, as suggested in recent studies.[4,16,18]

This type of heterogeneous reaction is likely to be a source of aldehydes and other oxygenated species to the atmosphere. In particular, carboxylic acids are formed, in agreement with the work of Eliason et al.,[14] via a mechanism that has to be confirmed. Yet to be quantified, this source could probably reduce the discrepancy between measured and predicted values of CH_3CHO and HCOOH ambient concentrations.[9,42] Finally, it should be noted that a similar kind of heterogeneous oxidation could occur not only at aerosol interfaces but also with the organic-rich microlayer found on the top of natural waters.

Acknowledgment. This work was supported by NSERC and acknowledgment is also made to the Donors of the American Chemical Society Petroleum Research Fund for support of this research. The PTR-MS was made available via infrastructure support to the Southern Ontario Centre for Atmospheric Aerosol Research from CFI, OIT, and ORF.

References and Notes

(1) Cooper, P. L.; Abbatt, J. P. D. *J. Phys. Chem.* **1996**, *100*, 2249−2254.

(2) Bertram, A. K.; Ivanov, A. V.; Hunter, M.; Molina, L. T.; Molina, M. J. *J. Phys. Chem. A* **2001**, *105*, 9415−9421.

(3) Hearn, J. D.; Smith, G. D. *Geophys. Res. Lett.* **2006**, *33*, L17805, doi:10.1029/2006GL026963.

(4) George, I. J.; Vlasenko, A.; Slowik, J. G.; Abbatt, J. P. D. *Atmos. Chem. Phys.* **2007**, *7*, 4187−4201.

(5) Lambe, A. T.; Zhang, J. Y.; Sage, A. M.; Donaghue, N. M. *Environ. Sci. Technol.* **2007**, *41*, 2357−2363.

(6) McNeill, V. F.; Wolfe, G. M.; Thornton, J. A. *J. Phys. Chem. A* **2007**, *111*, 1073−1083.

(7) Ellison, G. B.; Tuck, A. F.; Vaida, V. *J. Geophys. Res.-Atmos.* **1999**, *104*, 11633−11641.

(8) Robinson, A. L.; Donahue, N. M.; Rogge, W. F. *J. Geophys. Res.-Atmos.* **2006**, *111*, D03302, doi:10.1029/2005JD006265.

(9) Kwan, A. J.; Crounse, J. D.; Clarke, A. D.; Shinozuka, Y.; Anderson, B. E.; Crawford, J. H.; Avery, M. A.; McNaughton, C. S.; Brune, W. H.; Singh, H. B.; Wennberg, P. O. *Geophys. Res. Lett.* **2006**, *33*, L15815, doi:10.1029/2006GL026144.

(10) Molina, M. J.; Ivanov, A. V.; Trakhtenberg, S.; Molina, L. T. *Geophys. Res. Lett.* **2004**, *31*, L22104, doi:10.1029/2004GL020910.

(11) Mulcahy, M. F. R.; Young, B. C. *Carbon* **1975**, *13*, 115−124.

(12) Moise, T.; Rudich, Y. *Geophys. Res. Lett.* **2001**, *28*, 4083−4086.

(13) Moise, T.; Talukdar, R. K.; Frost, G. J.; Fox, R. W.; Rudich, Y. *J. Geophys. Res.-Atmos.* **2002**, 107.

(14) Eliason, T. L.; Gilman, J. B.; Vaida, V. *Atmos. Environ.* **2004**, *38*, 1367−1378.

(15) Lim, Y. B.; Ziemann, P. J. *Environ. Sci. Technol.* **2005**, *39*, 9229−9236.

(16) Docherty, K. S.; Ziemann, P. J. *J. Phys. Chem. A* **2006**, *110*, 3567−3577.

(17) Knopf, D. A.; Mak, J.; Gross, S.; Bertram, A. K. *Geophys. Res. Lett.* **2006**, *33*, L17816, doi:10.1029/2006GL026884.

(18) Hearn, J. D.; Renbaum, L. H.; Wang, X.; Smith, G. D. *Phys. Chem. Chem. Phys.* **2007**, *9*, 4803−4813.

(19) Mak, J.; Gross, S.; Bertram, A. K. *Geophys. Res. Lett.* **2007**, *34*, L10804, doi:10.1029/2007GL029756.

(20) Finlayson-Pitts, B. J.; Pitts, J. N. *Chemistry of Upper and Lower Atmosphere. Theory, Experiments, and Applications*; Academic Press: New York, 2000.

(21) Schmidt, M. W. I.; Masiello, C. A.; Skjemstad, J. O. *EOS* **2003**, *84*, 582.

(22) Thornberry, T.; Abbatt, J. P. D. *Phys. Chem. Chem. Phys.* **2004**, *6*, 84−93.

(23) Frinak, E. K.; Abbatt, J. P. D. *J. Phys. Chem. A* **2006**, *110*, 10456−10464.

(24) Aubin, D. G.; Abbatt, J. P. *Environ. Sci. Technol.* **2006**, *40*, 179−187.

(25) Sander, S. P.; Friedl, P. R.; Ravishankara, A. R.; Golden, D. M.; Kolb, C. E.; Kurylo, M. J.; Molina, M. J.; Moortgat, G. K.; Finlayson-Pitts, B. J.; Wine, P. H.; Huie, R. E.; Orkin, V. L.; *Chemical Kinetics and Photochemical Data for Use in Atmospheric Studies*, Evaluation Number 15; JPL Publication 06-2; NASA Jet Propulsion Laboratory: Pasadena, CA, 2006.

(26) Lovejoy, E. R.; Murrells, T. P.; Ravishankara, A. R.; Howard, C. J. *J. Phys. Chem.* **1990**, *94*, 2386−2393.

(27) Huey, L. G.; Hanson, D. R.; Howard, C. J. *J. Phys. Chem.* **1995**, *99*, 5001−5008.

(28) Lindinger, W.; Hansel, A.; Jordan, A. *Int. J. Mass Spectrom.* **1998**, *173*, 191−241.

(29) Chao, J.; Zwolinski, B. J. *J. Phys. Chem. Ref. Data* **1978**, *7*, 363−377.

(30) Sokolov, O.; Abbatt, J. P. D. *J. Phys. Chem. A* **2002**, *106*, 775−782.

(31) Andersen, M. P. S.; Stenby, C.; Nielsen, O. J.; Hurley, M. D.; Ball, J. C.; Wallington, T. J.; Martin, J. W.; Ellis, D. A.; Mabury, S. A. *J. Phys. Chem. A* **2004**, *108*, 6325−6330.

(32) Moortgat, G. K.; Veyret, B.; Lesclaux, R. *Chem. Phys. Lett.* **1989**, *160*, 443−447.

(33) Tyndall, G. S.; Cox, R. A.; Granier, C.; Lesclaux, R.; Moortgat, G. K.; Pilling, M. J.; Ravishankara, A. R.; Wallington, T. J. *J. Geophys. Res.-Atmos.* **2001**, *106*, 12157−12182.

(34) Chameides, W. L.; Davis, D. D. *Nature* **1983**, *304*, 427−429.

(35) Hansel, A.; Wisthaler, A. *Geophys. Res. Lett.* **2000**, *27*, 895−898.

(36) Atkinson, R. *Chem. Rev.* **1986**, *86*, 69−201.

(37) Aschmann, S. M.; Arey, J.; Atkinson, R. *J. Phys. Chem. A* **2001**, *105*, 7598−7606.

(38) Reisen, F.; Aschmann, S. M.; Atkinson, R.; Arey, J. *Environ. Sci. Technol.* **2005**, *39*, 4447−4453.

(39) Picquet-Varrault, B.; Doussin, J. F.; Durand-Jolibois, R.; Carlier, P. *J. Phys. Chem. A* **2002**, *106*, 2895−2902.

(40) Sasaki, J.; Aschmann, S. M.; Kwok, E. S. C.; Atkinson, R.; Arey, J. *Environ. Sci. Technol.* **1997**, *31*, 3173−3179.

(41) Atkinson, R.; Arey, J. *Polycycl. Aromat. Compd.* **2007**, *27*, 15−40.

(42) Baboukas, E. D.; Kanakidou, M.; Mihalopoulos, N. *J. Geophys. Res.-Atmos.* **2000**, *105*, 14459−14471.